

Enhanced Specific Activity by Multichelation of Exendin-3 Leads To Improved Image Quality and *In Vivo* Beta Cell Imaging

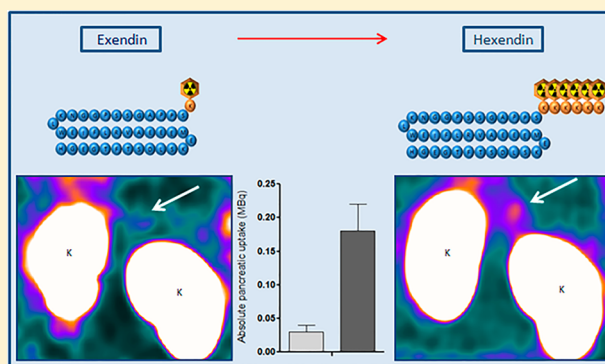
Lieke Joosten,^{*,†} Maarten Brom,[†] Hanneke Peeters,^{†,§} Sandra Heskamp,[†] Martin Béhé,[‡] Otto Boerman,[†] and Martin Gotthardt[†]

[†]Department of Radiology and Nuclear Medicine, Radboud University Medical Center, PO Box 9101, 6500 HB Nijmegen, The Netherlands

[‡]Center for Radiopharmaceutical Sciences ETH-PSI-USZ, Paul Scherrer Institut, 5232 Villigen, Switzerland

ABSTRACT: Glucagon-like peptide-1 receptor (GLP-1R) targeting using radiolabeled exendin is a promising approach to noninvasively visualize and determine beta cell mass (BCM), which could help to unravel the pathophysiology of diabetes. However, saturation of the GLP-1R on beta cells occurs at low peptide doses, since the number of receptors expressed under physiological conditions is low. Therefore, tracers with high specific activities are required to sensitively image small variations in BCM. Here, we describe a novel exendin-3-based radiotracer with multiple chelators and determine its potential for *in vivo* beta cell imaging. Exendin-3 was modified by adding six lysine residues C-terminally conjugated with one, two, or six DTPA moieties. All compounds were labeled with ¹¹¹In and their GLP-1R affinity was determined *in vitro* using GLP-1R expressing cells. The *in vivo* behavior of the ¹¹¹In-labeled tracers was examined in BALB/c nude mice with a subcutaneous GLP-1R expressing tumor (INS-1). Brown Norway rats were used for SPECT visualization of the pancreatic BCM. Addition of six lysine and six DTPA residues (hexendin(40–45)) resulted in a 7-fold increase in specific activity (from 0.73 GBq/nmol to 5.54 GBq/nmol). IC₅₀ values varied between 5.2 and 69.5 nM. All compounds with two or six lysine and DTPA residues had a significantly lower receptor affinity than [Lys⁴⁰(DTPA)]exendin-3 (4.4 nM, *p* < 0.05). The biodistribution in mice revealed no significant decrease in pancreatic uptake after addition of six lysine and DTPA molecules. Hexendin(40–45) showed a 6-fold increase in absolute ¹¹¹In uptake in the pancreas of Brown Norway rats compared to [Lys⁴⁰(DTPA)]exendin-3 (182.7 ± 42.3 kBq vs 28.8 ± 6.0 kBq, *p* < 0.001). Visualization of the pancreas on SPECT was improved using hexendin(40–45), due to the higher count rate, achieved at the same peptide dose. In conclusion, hexendin(40–45) showed an improved visualization of the pancreas with SPECT. This tracer holds promise to sensitively and specifically detect small variations in BCM.

KEYWORDS: beta cells, exendin, radiolabeling, specific activity, SPECT



INTRODUCTION

Currently, 422 million people worldwide are suffering from diabetes, and it is expected that this number will have doubled by 2030.¹ These dramatic numbers underline the importance for research aiming to improve diagnosis and treatment of the disease. Gaining better insight into the pathophysiology of the different types of diabetes is therefore one of the major goals of current diabetes research.

The diagnosis of diabetes is currently based on laboratory tests, such as blood glucose measurements and oral glucose tolerance testing. However, they do not provide information about the underlying pathophysiological processes and can only detect the downstream consequences (i.e., impaired glucose tolerance) of processes that have started years before diagnosis. Currently, the loss of beta cell mass (BCM) and beta cell function (not being directly related to mass) proceeding to overt hyperglycaemia is gaining attention and determination of BCM has emerged as a field of diabetes research.² To date,

biopsy and autopsy studies of diabetic patients are the only source of information regarding BCM. However, this only provides information at one time point³ and pancreatic biopsies in T1D patients have been shown to be associated with a high rate of serious complications.⁴ Therefore, there is a clear need for a noninvasive method to measure the loss of BCM in individual patients. A promising approach addressing this urgent issue would be a sensitive, specific, and noninvasive imaging method to detect viable beta cells in the pancreas, which would also enable determination of the exact relation between the BCM and beta cell function during the course of the disease.^{5,6} The high technological demands for *in vivo* beta cell imaging and the need for a highly sensitive and specific

Received: September 28, 2017

Revised: November 20, 2017

Accepted: December 11, 2017

Published: December 11, 2017

Table 1. Amino Acid Sequence of ZP10A, Exendin-4, Exendin-3, and GLP1^a

peptide	amino acid sequence
poly-lysine-exendin-4 (ZP10A) ¹⁶	HGEGTFTSDLSKQMEEEEAVRLFIEWLKNNGPSSGAPPPSKKKKK-NH ₂
exendin-4	HGEGTFTSDLSKQMEEEEAVRLFIEWLKNNGPSSGAPPPS-NH ₂
exendin-3	HSDGTFTSDLSKQMEEEEAVRLFIEWLKNNGPSSGAPPPS-NH ₂
GLP-1	HAEGTFTSDVSSYLEGQAAKEFIAWLVKGRG-NH ₂

^aAmino acids homologous to GLP-1 are in bold.

imaging method displaying a high target-to-background ratio have been discussed extensively in the literature.^{5,7–10} Namely, the low amount of beta cells (only a few gram) and the diffuse distribution throughout the pancreas represent a major challenge for *in vivo* imaging.⁶ Recently, it has been shown that radiolabeled exendin is a promising tracer to visualize pancreatic beta cells *in vivo* in rodents and humans.^{6,11} Exendin-3 is an analogue of GLP-1 (glucagon-like peptide-1) and binds with high affinity to the GLP-1 receptor (GLP-1R) which is specifically expressed on the pancreatic beta cells as well as on beta cell derived tumors.^{12,13} In order to improve image quality, enabling better delineation of the pancreas (which can be hampered by the proximity of the kidneys accumulating radioactivity), higher uptake of radiolabeled exendin-3 in the pancreas is warranted to obtain optimal count rates and high signal-to-background ratios. Since the GLP-1R is expressed at relatively low levels on beta cells in healthy rodents (as compared to for example neuroendocrine tumors massively overexpressing somatostatin receptors) and the total BCM is decreased in diabetic animals, the receptor is saturated at comparably low peptide doses. It has been demonstrated that the maximum peptide dose for exendin imaging of pancreatic beta cells in mice and rats is 20 pmol per injection.^{14,15} In order to achieve optimal SPECT image quality, labeling of exendin with very high specific activities is required.

Previously, an exendin analogue with six extra lysine residues at the C-terminus has been described (Table 1).¹⁶ The addition of lysine residues would theoretically allow the conjugation of multiple DTPA moieties to produce a tracer with a higher specific activity. In the present study, we have tested five novel variants of exendin-3 by adding multiple DTPA moieties to the C-terminal lysine residues and we evaluated whether (1) the specific activity would be enhanced, (2) the modifications would influence the affinity for the GLP-

1R, (3) targeting to beta cells would be increased (in terms of absolute radioactivity concentration), and (4) image quality would be improved.

■ MATERIALS AND METHODS

Peptides and Radionuclides. ¹¹¹InCl₃ was obtained from Mallinckrodt Medical (Petten, The Netherlands) and the DTPA-exendin-3 peptides were purchased from Peptide Specialty Laboratories (PSL, Heidelberg, Germany). The exendin-3 compounds with 6 additional lysine residues are referred to as hexendin (hexa-lysine-exendin-3) hereafter. One or multiple DTPA molecules were conjugated to the ε-amino group of C-terminal lysines at different positions. The structure, names, and molecular weights of the peptides are shown in Table 2. Exendin-3, with DTPA conjugated to lysine at position 40 ([Lys⁴⁰(DTPA)]exendin-3), was used as the reference in this study.

Radiolabeling of DTPA-Exendin-3 Analogues with ¹¹¹In. The peptides were dissolved in metal-free 0.1 M MES (2-(*N*-morpholino) ethanesulfonic acid, Sigma-Aldrich, St. Louis, MO, USA), pH 5.5.¹⁷ ¹¹¹InCl₃ was added to 0.1 M MES buffer, pH 5.5, containing the respective peptide: One volume of ¹¹¹InCl₃ was mixed with two volumes of MES buffer. After incubation for 20 min at room temperature, 50 mM EDTA (ethylenediaminetetraacetic acid) (Sigma-Aldrich) was added to a final concentration of 5 mM. Subsequently, 10% Tween-80 (Sigma-Aldrich) in PBS was added to a final concentration of 0.1% to prevent sticking of the peptide to the reaction vial. The maximum specific activity of each analogue was determined by performing a series of radiolabeling reactions ranging from 75 to 300 MBq for [Lys⁴⁰(DTPA)]-exendin-3, hexendin(40), hexendin(45), and hexendin(40 + 45) (200 pmol of peptide was added to the reaction mixture) and 75 to 900 MBq for hexendin(40 + 41) and hexendin(40–45) (100 pmol of peptide was added to the reaction mixture).

Table 2. Structure, Name, and Molecular Mass of Exendin-3 Derivatives^a

peptide	amino acid sequence	molecular weight (Da)
[Lys ⁴⁰ (DTPA)]exendin-3	HSDGTFTSDLSKQMEEEEAVRLFIEWLKNNGPSS-GAPPPSK(DTPA)	4816.3
hexendin(40)	HSDGTFTSDLSKQMEEEEAVRLFIEWLKNNGPSS-GAPPPSK(DTPA)KKKKK	5345.7
hexendin(45)	HSDGTFTSDLSKQMEEEEAVRLFIEWLKNNGPSS-GAPPPSKKKKKK(DTPA)	5345.7
hexendin(40 + 45)	HSDGTFTSDLSKQMEEEEAVRLFIEWLKNNGPSS-GAPPPSK(DTPA)KKKKK(DTPA)	5720.8
hexendin(40 + 41)	HSDGTFTSDLSKQMEEEEAVRLFIEWLKNNGPSS-GAPPPSK(DTPA)K(DTPA)KKKK	5724.5
hexendin(40–45)	HSDGTFTSDLSKQMEEEEAVRLFIEWLKNNGPSS-GAPPPSK(DTPA)K(DTPA)K(DTPA)K(DTPA)K(DTPA)K(DTPA)	7235.6

^aThe lysine position to which DTPA is conjugated is indicated between parentheses (), the lysine residues and DTPA moieties attached are marked in bold.

Radiochemical purity was determined by instant thin layer chromatography on silica-gel strips (ITLC-SG Biodex, Shirley, NY, USA) using 0.1 M EDTA in 0.1 M NH_4Ac as a mobile phase (R_f ^{111}In -labeled peptides = 0, R_f ^{111}In -EDTA = 1).

The labeled peptides were purified by solid-phase extraction using an HLB (hydrophilic–lipophilic balance reversed-phase sorbent) cartridge (Waters Oasis, Milford, MA, USA) as described previously.¹⁸ For conditioning and washing of the cartridge, 1 mL 0.1 M MES was used.

Cell Culture. For *in vivo* experiments the rat insulinoma cell line INS-1 was used.¹⁹ INS-1 cells were cultured in RPMI-1640 medium supplemented with 10% fetal calf serum, 2 mM glutamine, 100 units/ml penicillin, 100 $\mu\text{g}/\text{mL}$ streptomycin, 10 mM HEPES, 50 μM β -mercaptoethanol, and 1 mM sodiumpyruvate. CHL-cells transfected with the human GLP-1 receptor (a kind gift of Brigitte Lankat-Buttgereit, Marburg) were used for the *in vitro* experiments. CHL-GLP-1R cells were maintained in Dulbecco's Modified Eagle's Medium (DMEM) GlutaMAX (Gibco, Invitrogen, Breda, The Netherlands), supplemented with 10% fetal calf serum, 100 units/ml penicillin, 100 $\mu\text{g}/\text{mL}$ streptomycin, Geneticin (G418) sulfate solution (0.5 mg/mL final concentration), 1 mM sodiumpyruvate, and 0.1 mM nonessential amino acids. Cells were maintained in a humidified 5% CO_2 atmosphere at 37 °C.

Competitive Binding Assay. The relative affinity of the exendin analogs for the GLP-1R was determined in a competitive binding assay using CHL-GLP-1R cells. CHL-GLP-1R cells were seeded in six-well plates at 1×10^6 cells/well 2 days prior to the experiment. All peptides were labeled with ^{111}In . A 5-fold molar excess of ^{111}In prepared in 0.02 M HCl was added to the peptides and two volumes of 0.1 M MES buffer. After incubation at room temperature for 20 min, 10% Tween-80 was added to a final concentration of 0.1%. Serial dilutions of these “cold-labeled” compounds were prepared in DMEM GlutaMAX with 0.5% *w/v* BSA (bovine serum albumin). Cells were washed once with GlutaMAX with 0.5% *w/v* BSA and the “cold-labeled” peptides were added at a final concentration ranging from 0.1 to 1000 nM along with 1 kBq (1.4 fmol) ^{111}In -labeled [Lys⁴⁰(DTPA)]exendin-3. After incubation on ice for 4 h, cells were washed with ice-cold GlutaMAX with 0.5% *w/v* BSA and the cells were harvested with 0.1 M NaOH. Cell-associated radioactivity was determined in a γ -counter (Wallac 1480-Wizard, PerkinElmer, Boston, MA, USA) and the IC_{50} (half-maximal inhibitory concentration) was calculated using GraphPad Prism (version 5.03, GraphPad Software, San Diego California USA).

Biodistribution at Equimolar Doses. All animal experiments were performed according to national laws and regulations and approved by the animal welfare body of the Radboud University. To examine the *in vivo* GLP-1R targeting properties of the ^{111}In -labeled exendin analogs, six to eight weeks old female BALB/crJ nu mice (Janvier, Saint-Berthevin, France) were inoculated subcutaneously with 1×10^7 INS-1 cells in 200 μL RPMI medium. Mice were randomly divided into 12 groups ($n = 5$ per group). Each group was injected intravenously with 0.1–0.7 MBq of one of the following ^{111}In -labeled peptides: [Lys⁴⁰(DTPA)]exendin-3, hexendin(40), hexendin(45), hexendin(40 + 45), hexendin(40 + 41), or hexendin(40–45). Equimolar doses of the labeled analogues were administered (20 pmol) to the mice. For each analogue, an additional group of 5 mice was co-injected with an excess (2 nmol) of unlabeled Lys⁴⁰exendin-3 to determine the biodistribution of the tracer while blocking the GLP-1

receptors *in vivo*. After 2 h, mice were euthanized by CO_2/O_2 asphyxiation. Relevant organs were dissected, weighed, and counted in a γ -counter. For each tissue sample the uptake was calculated and presented as the percentage of the injected dose per gram tissue (%ID/g).

Biodistribution at Different Molar Doses. Because hexendin(40 + 41) and hexendin(40–45) can be labeled at higher specific activities, it allows injection of a lower peptide dose. To investigate whether administering a lower peptide dose could lead to higher uptake of the tracer in the target tissue (in terms of %ID/g), BALB/c nude mice with a s.c. INS-1 tumor were injected with 4 pmol of hexendin(40 + 41) or hexendin(40–45) and compared to injection of 20 pmol of [Lys⁴⁰(DTPA)]exendin-3. For all compounds 0.2 MBq of the ^{111}In -labeled peptide was injected. To determine the non-GLP-1R mediated biodistribution of the tracers, for each peptide an additional group of 5 mice was co-injected with an excess (2 nmol) of unlabeled Lys⁴⁰exendin-3. The *ex vivo* biodistribution was performed as described above.

SPECT. To compare the ability of the tracers to visualize GLP-1R expressing cells in the pancreas, SPECT studies were carried out in male Brown Norway (BN) rats. Two groups of rats ($n = 5$) received 19.4 ± 1.3 MBq (20 pmol) of either ^{111}In -labeled [Lys⁴⁰(DTPA)]exendin-3 or hexendin(40–45). An additional group received ^{111}In -hexendin(40–45) at a 7.5-fold higher activity dose (20 pmol, 149.1 ± 3.8 MBq ($n = 4$)) to investigate the effect of the activity dose on the image quality. SPECT scans were acquired under isoflurane/ O_2 anesthesia 2 h after injection of the radiolabeled peptide using a dedicated small animal SPECT/CT scanner (U-SPECT-II, MILabs, Utrecht, The Netherlands). Images were acquired for 50 min, using a 1.0 mm multipinhole general purpose mouse and rat collimator. Rats were euthanized by CO_2/O_2 asphyxiation and the *ex vivo* biodistribution was determined as described above. Absolute uptake in the pancreas and kidneys was calculated by multiplying the injected dose (MBq) by the uptake in the organs (percent injected dose in the total dissected organ).

Images were reconstructed using the U-SPECT-Rec Software (MILabs, Utrecht, The Netherlands). Inveon Research Workplace (Preclinical Solutions, Siemens Medical Solutions USA, Inc., Knoxville, TN, USA) was used to quantify the pancreatic uptake of the ^{111}In -labeled peptides by drawing a volume of interest over the pancreas and in the abdomen (below the kidneys) as a background region. The image quality was determined quantitatively by calculating the ratio of the mean activity in the pancreas region and the activity in the background region (signal-to-background ratio).²⁰

Statistical Analysis. Data were analyzed using GraphPad Prism software version 5.03 for Windows. One-way ANOVA followed by a Tukey test was used to determine significance. A *p*-value below 0.05 was considered significant. For the competitive binding assay the F-test was used to manually calculate significance.

RESULTS

Specific Activity. The maximum specific activity of the ^{111}In -labeled exendin analogues and the theoretical maximum specific activity (assuming all DTPA-molecules chelating ^{111}In) are summarized in Table 3. For all tracers the radiochemical purity exceeded 99% after purification. The specific activity of [Lys⁴⁰(DTPA)]exendin-3 (0.73 GBq/nmol) was similar to

Table 3. Maximum and Theoretical Specific Activity of Exendin-3 Derivatives^a

compound	maximum specific activity achieved (GBq/nmol)	maximum theoretical specific activity (GBq/nmol)
[Lys ⁴⁰ (DTPA)]exendin-3	0.73	1.72
hexendin(40)	0.69	1.72
hexendin(45)	0.67	1.72
hexendin(40 + 41)	1.66 ^b	3.44
hexendin(40 + 45)	1.32	3.44
hexendin(40–45)	5.54	10.33

^aThe maximum theoretical specific activity calculated for exendin-3, conjugated with one, two, or six DTPA molecules, with the assumption that 1 nmol of ¹¹¹In will be complexed in 1 nmol of DTPA. ^bThe labeling is not reproducible, and varies from 0.85 GBq/nmol to 4.24 GBq/nmol.

that of the exendin-3 analogues with 6 lysine residues and only one DTPA attached (hexendin(40) and hexendin(45): 0.69 and 0.67 GBq/nmol). The specific activity of hexendin(40 + 41) and hexendin(40 + 45) was approximately 2-fold higher (1.66 and 1.32 GBq/nmol, respectively) compared to the reference peptide. Finally, hexendin(40–45) could be labeled with a specific activity of 5.54 GBq/nmol, which is 7.5-times higher than that of the reference peptide. Furthermore, the radiolabeling of [Lys⁴⁰(DTPA)]exendin-3 resulted in 42% of the theoretical maximum specific activity, whereas 54% of the theoretical maximum specific activity was reached for hexendin(40–45).

Competitive Binding Assay. In Figure 1 the results of the competitive binding assay on CHL-GLP-1R cells are shown.

The IC₅₀ values of all peptides were in the low nanomolar range. The IC₅₀ of hexendin(40) and hexendin(45) were 5.2 and 6.3 nM, respectively. The IC₅₀ of hexendin(40 + 45), hexendin(40 + 41), and hexendin(40–45) were 10.1, 19.2, and 69.5 nM, respectively. All peptides, except hexendin(40), had a significantly lower affinity for the receptor than the reference peptide (4.4 nM, *p* < 0.05).

Biodistribution at Equimolar Doses. Figure 2 shows the biodistribution of all ¹¹¹In-labeled exendin analogues (at a peptide dose of 20 pmoles) in BALB/c nude mice with a subcutaneous INS-1 tumor 2 h post injection. [Lys⁴⁰(DTPA)]exendin-3, showed the highest uptake (33.8 ± 7.6%ID/g) in the INS-1 tumor. C-terminal addition of six lysine residues (hexendin(40)) reduced the tumor uptake to 19.8 ± 5.8%ID/g (*p* < 0.05). Conjugation of multiple DTPA molecules did not affect the tumor uptake significantly compared to hexendin(40) (hexendin(40 + 45): 15.9 ± 1.3%ID/g, hexendin(40 + 41): 22.9 ± 7.3%ID/g, hexendin(40–45): 19.9 ± 9.2%ID/g). The pancreatic uptake of hexendin(40) (7.60 ± 1.50%ID/g) was lower than that of [Lys⁴⁰(DTPA)]exendin-3 (11.97 ± 4.04%ID/g). Hexendin with two or more DTPA molecules showed similar pancreatic uptake as [Lys⁴⁰(DTPA)]exendin-3: hexendin(40 + 41) (10.77 ± 2.87%ID/g) and hexendin(40–45) (9.77 ± 2.72%ID/g). Accumulation in the tumor and the pancreas could be blocked by an excess of unlabeled exendin-3, proving GLP-1R mediated uptake for all compounds. Furthermore, the lungs, stomach, and duodenum also showed receptor-mediated uptake of exendin-3. Renal uptake of all peptides was high and could not be blocked by an excess of unlabeled exendin-3.

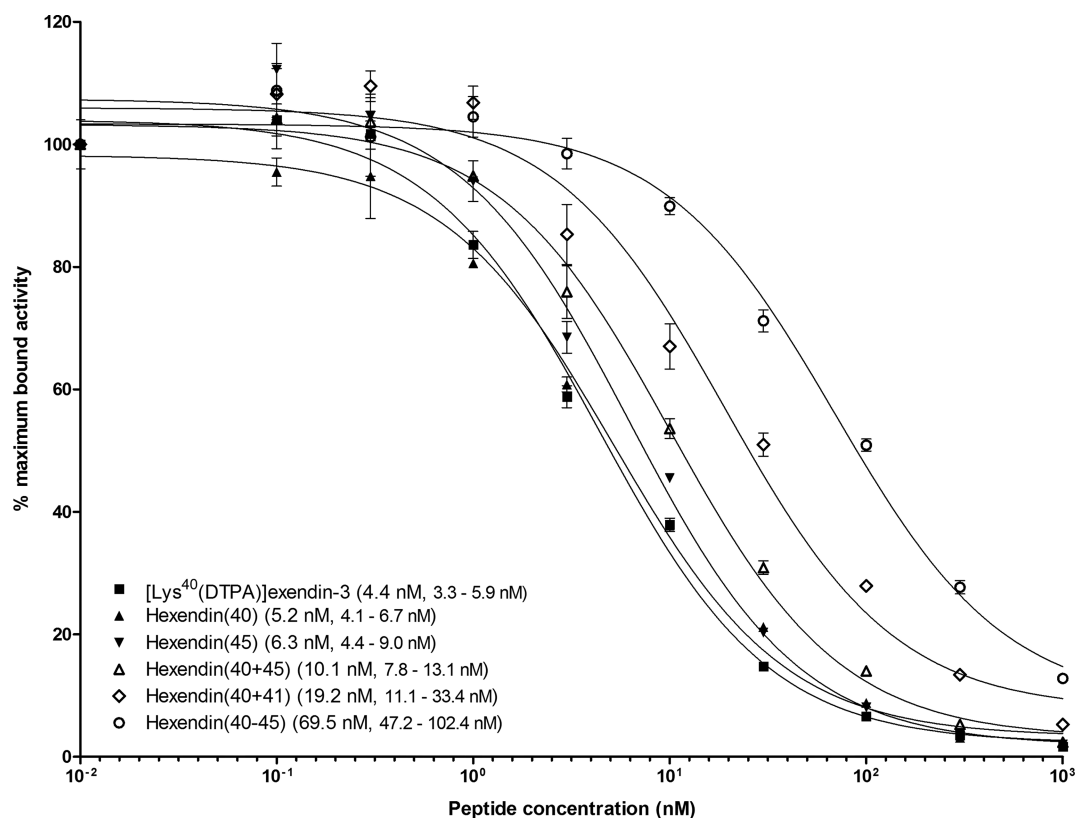


Figure 1. Curves of the competitive binding assay (IC₅₀) on CHL-GLP1R cells. ¹¹¹In-labeled [Lys⁴⁰(DTPA)]exendin-3 was used as radiotracer. The IC₅₀ values and 95% confidence intervals in nM are given between parentheses ().

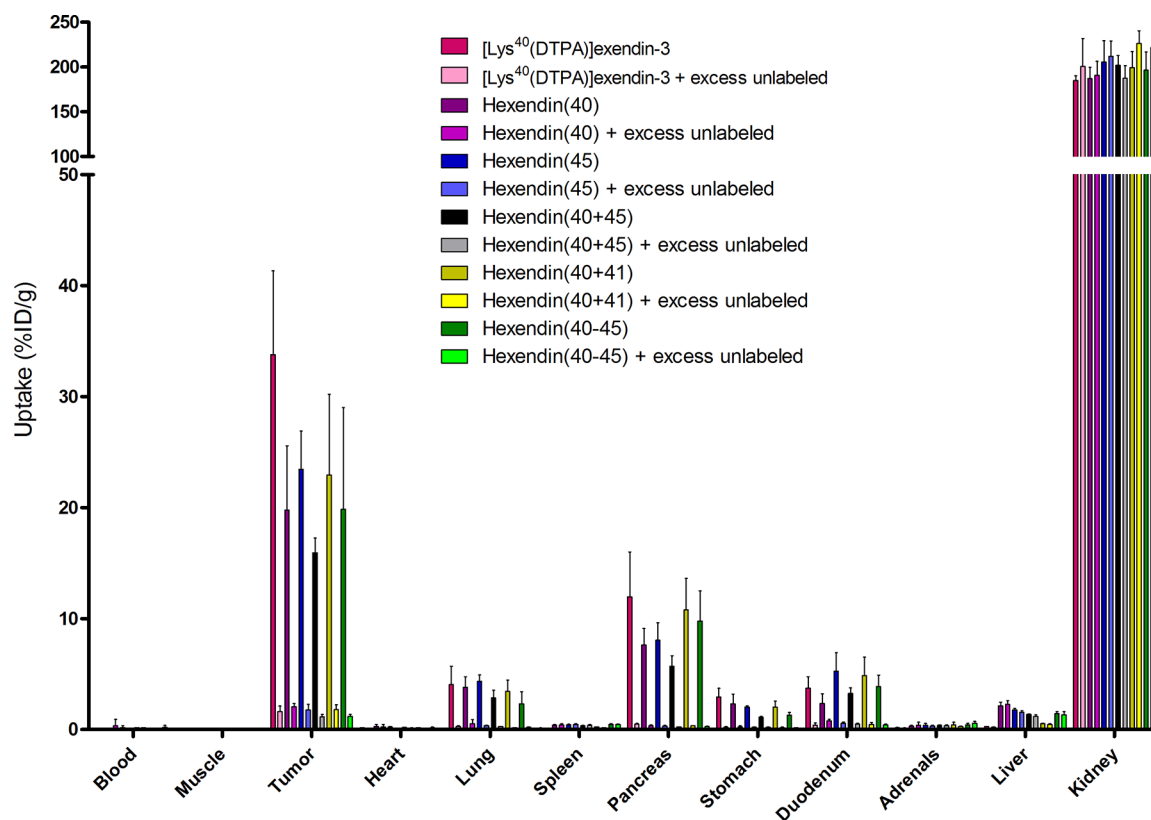


Figure 2. Biodistribution of ^{111}In -labeled exendin-3 derivatives in BALB/c nude mice bearing a subcutaneous INS-1 tumor. Values are expressed as a percentage of the injected dose per gram of tissue ($n = 5$ mice per group, error bars SD).

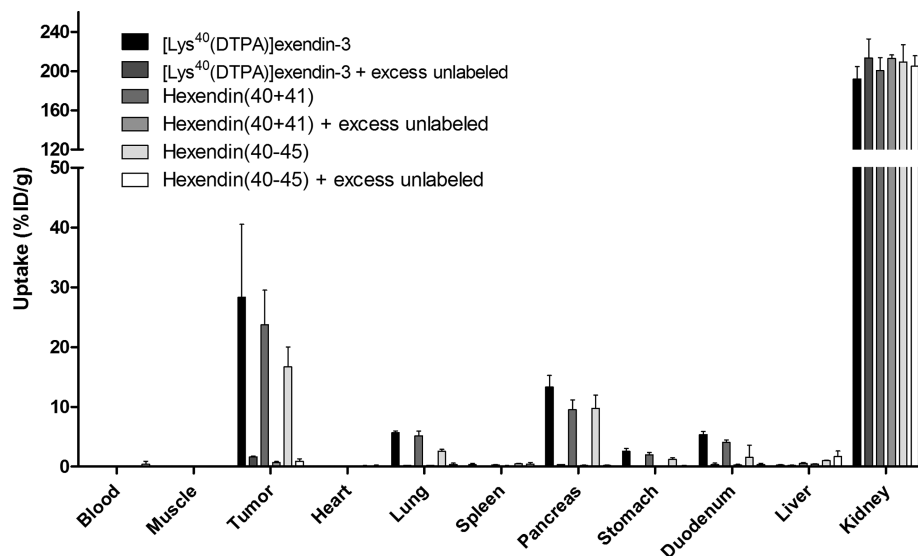


Figure 3. Biodistribution of ^{111}In -labeled $[\text{Lys}^{40}(\text{DTPA})]$ exendin-3 (20 pmol), hexendin(40 + 41) (4 pmol), and hexendin(40–45) (4 pmol) in BALB/c nude mice with a subcutaneous INS-1 tumor. Values are expressed as %ID/g ($n = 5$ mice per group, error bars SD).

Biodistribution at Different Molar Doses. In order to assess whether the uptake of the tracer in the pancreas could be further enhanced by reducing the administered peptide dose, the biodistribution of 20 pmol of the reference peptide was compared to that of 4 pmol of hexendin(40 + 41) and hexendin(40–45) (Figure 3). When the standard $[\text{Lys}^{40}(\text{DTPA})]$ exendin-3 dose of 20 pmol was given, the uptake in tumor was $28.3 \pm 12.2\% \text{ID/g}$. A peptide dose of 4 pmol resulted in a tumor uptake of 23.7 ± 5.8 and $16.7 \pm 3.3\%$

ID/g, respectively, for hexendin(40 + 41) and hexendin(40–45), which was not significantly different. Pancreatic uptake was $13.3 \pm 1.9\% \text{ID/g}$ for $[\text{Lys}^{40}(\text{DTPA})]$ exendin-3 at the standard peptide dose, while this was 9.5 ± 1.7 and $9.8 \pm 2.2\% \text{ID/g}$ for hexendin(40 + 41) ($p < 0.05$) and hexendin(40–45) ($p < 0.05$), respectively, at a peptide dose of 4 pmol. Renal uptake did not change significantly.

SPECT. Addition of multiple DTPA molecules allowed for labeling at a higher specific activity. Therefore, in the final

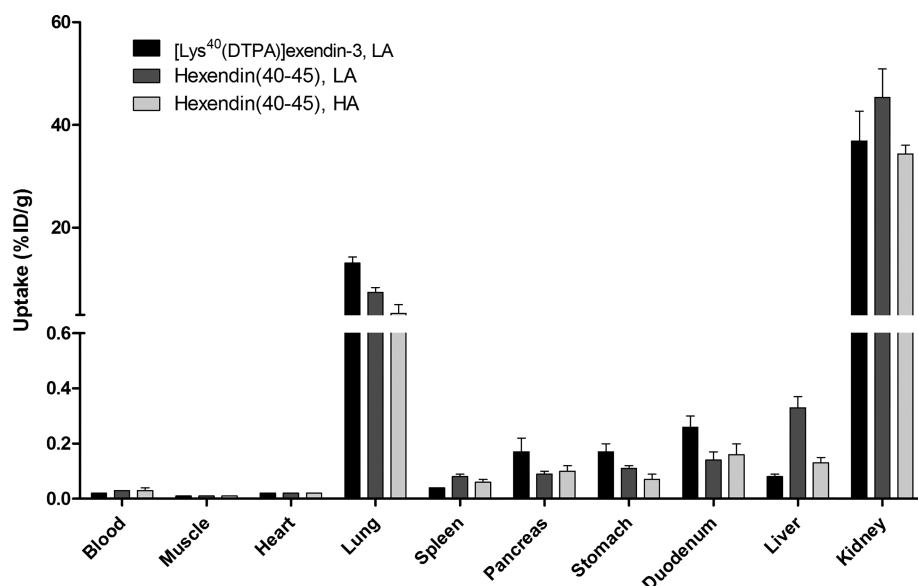


Figure 4. Biodistribution of ^{111}In -labeled $[\text{Lys}^{40}(\text{DTPA})]$ exendin-3 and hexendin(40–45) in Brown Norway rats. Values are expressed as %ID/g ($n = 5$ rats per group for the LA (low activity) and $n = 4$ rats per group for the HA (high activity), error bars SD).

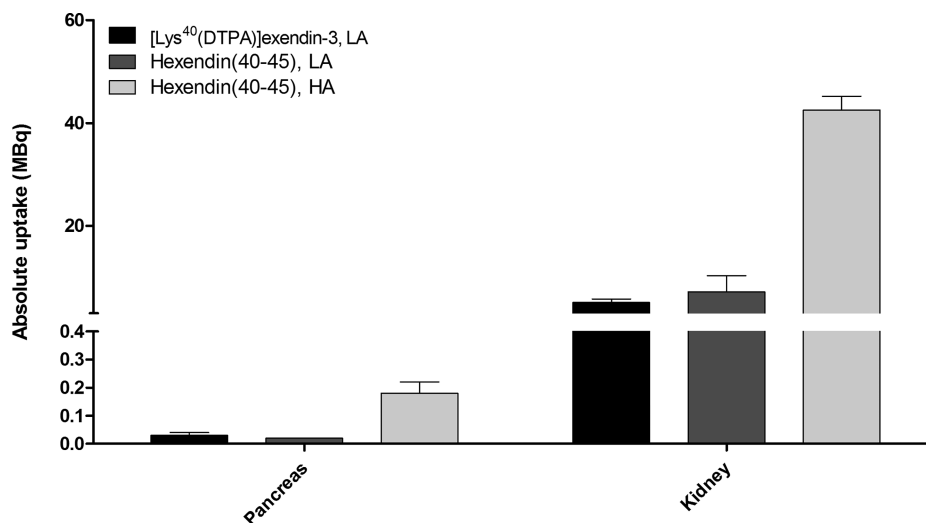


Figure 5. Absolute uptake of ^{111}In -labeled $[\text{Lys}^{40}(\text{DTPA})]$ exendin-3 and hexendin(40–45) in pancreas and kidney.

experiment, we labeled hexendin(40–45) at a high specific activity and we investigated whether visualization of the pancreas with SPECT could be improved by administering a higher activity dose (at equimolar peptide doses), compared to labeling of hexendin(40–45) or $[\text{Lys}^{40}(\text{DTPA})]$ exendin-3 at a low specific activity. Figure 4 shows the biodistribution profiles of $[\text{Lys}^{40}(\text{DTPA})]$ exendin-3 and hexendin(40–45) in BN rats. Pancreatic uptake was higher for $[\text{Lys}^{40}(\text{DTPA})]$ exendin-3 ($0.17 \pm 0.05\% \text{ID/g}$) than for hexendin(40–45), either labeled at a low (LA) or high (HA) specific activity (0.09 ± 0.01 ($p < 0.01$) and $0.10 \pm 0.02\% \text{ID/g}$ ($p < 0.05$), respectively). The absolute uptake in pancreas and kidneys was assessed for all three tracers and is shown in Figure 5. The absolute pancreatic uptake of $[\text{Lys}^{40}(\text{DTPA})]$ exendin-3 (28.8 ± 6.0 kBq) and hexendin(40–45) (19.9 ± 1.5 kBq) did not differ significantly, when labeled at the same specific activity. However, injection with a high activity dose of hexendin(40–45) resulted in an absolute uptake in the pancreas which was 9 times higher than injection of a low activity dose (182.7 ± 42.3 kBq compared to

19.9 ± 1.5 kBq, $p < 0.001$). The absolute renal uptake was 6-fold higher: 42.52 ± 2.68 MBq vs 7.17 ± 3.16 MBq ($p < 0.001$). Typical images of rats injected with $[\text{Lys}^{40}(\text{DTPA})]$ exendin-3 or hexendin(40–45), labeled at a low specific activity are shown in Figure 6a and b. The image quality improved when hexendin(40–45) with a high specific activity was administered (Figure 6c). The pancreas-to-background ratio (Figure 7) increased to 18.8 ± 4.3 for hexendin(40–45) (HA), compared to 6.6 ± 1.9 for $[\text{Lys}^{40}(\text{DTPA})]$ exendin-3 (LA) and 10.9 ± 2.2 for hexendin(40–45) (LA) ($p < 0.001$).

DISCUSSION

In this study, a novel exendin analogue was presented that can be labeled at a 7-fold higher specific activity as compared to $[\text{Lys}^{40}(\text{DTPA})]$ exendin-3. The relative pancreatic uptake of this new tracer with six lysine and DTPA moieties (expressed as %ID/g) in mice was comparable to that of the reference peptide, however, the absolute activity uptake of hexendin(40–45) in the pancreas was 9-fold higher. This increased

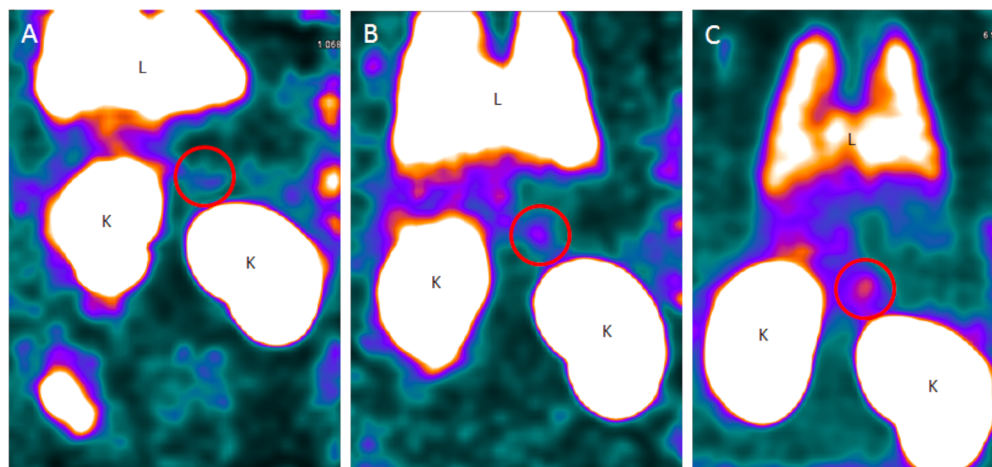


Figure 6. Coronal slices of SPECT images of Brown Norway rats, obtained two hours after injection of the peptide. (A) 20 pmol ^{111}In -labeled $[\text{Lys}^{40}(\text{DTPA})]\text{exendin-3}$ (19.1 ± 2.4 MBq), (B) 20 pmol ^{111}In -labeled hexendin(40–45) (18.4 ± 0.2 MBq), (C) 20 pmol ^{111}In -labeled hexendin(40–45) (149.1 ± 3.8 MBq). Lungs are indicated with L, kidneys with K, and the pancreas is delineated with a red circle.

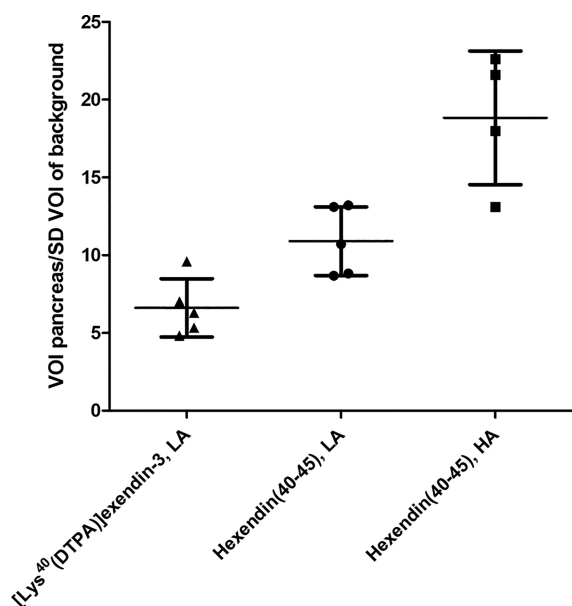


Figure 7. Signal-to-background ratio.

pancreas activity resulted in an almost 3-fold improvement of the signal-to-background ratio of the images and clearly improved pancreas visualization.

Breeman et al. optimized labeling conditions to reach higher specific activities to avoid receptor saturation or pharmacological (side) effects.²¹ When using optimal labeling conditions, like metal-free materials, appropriate temperatures, or buffers, still leaves room for improvement, a modification of the compound is an additional approach to enhance the specific activity.

Conjugation of five extra lysine residues to the C-terminus of $[\text{Lys}^{40}(\text{DTPA})]\text{exendin-3}$ allowed to attach multiple DTPA moieties. The $^{111}\text{InCl}_3$ incorporation in hexendin(40–45) was 20 percent more efficient, relatively, than in the reference peptide, leading to a very clear absolute increase in specific activity from 0.73 GBq/nmol to 5.54 GBq/nmol.

The increased specific activity obtained in this study allowed us to administer either lower amounts of peptide or higher amounts of radioactivity at equal peptide doses of the tracer.

Although lowering the peptide dose did not lead to an increased relative accumulation in target tissues, injecting a higher amount of radioactivity led to enhanced absolute accumulation of radiolabeled exendin. Background activity increased to a lesser extent, resulting in improved target-to-background ratios and improved visualization of the pancreas on SPECT. This represents a clear improvement for *in vivo* imaging as low peptide doses of exendin should be administered to avoid receptor saturation;¹⁴ as stated previously, this is of even more importance for beta cell quantification in the pancreas of diabetic individuals with lower BCM and thus a lower number of GLP-1R available for binding.

Although administration of higher ligand doses may be possible in clinical studies, also for peptides or antibodies which are biologically active, like exendin, it is of great interest to administer low pharmacological doses to limit the potential (biological) side-effects of the tracer. Using the hexendin(40–45) for instance, the peptide dose administered to patients could be reduced almost seven times, thereby preventing side-effects, while maintaining a sufficient amount of radioactivity (150 MBq).

A disadvantage of multichelated compounds is the higher radioactivity accumulation in the kidneys. In preclinical imaging studies this is not a limiting factor, while in clinical studies this would result in unfavorably high radiation doses to the kidneys.

In our view, the multichelation approach presented here has high translational potential, because it is widely applicable, not only for different SPECT tracers, but also for PET tracers and other peptides or antibodies. When the labeling procedure of an antibody, for example, is restricted to a low temperature, the multichelation approach could help to improve the specific activity. In addition, several antibody-based imaging agents are also limited by the protein dose that can be administered without saturating the tumor-associated receptor (e.g., PD-L1, IGF-1R).^{22,23} Also, for evaluation of tracer molecules, this technology facilitates determination of optimal (low) tracer doses *in vivo*.

The concept of conjugating more than one chelator molecule to one mole of antibody was demonstrated almost three decades ago. In the respective study from Boniface et al.,

an increase in specific activity was found by increasing the cDTPA:mAb (monoclonal antibody) conjugation ratio.²⁴ A major difference between their study and the study presented here, is the conjugation method. When conjugating antibodies, the chelator moieties are randomly bound to the antibody, possibly in the binding domain and thereby influencing the affinity or immunoreactivity of the antibody. In the present study, the DTPA moieties were conjugated site-specifically to additional lysine residues. By F-moc protection of the lysines that should not be conjugated, random conjugation interference in the binding domain was prevented.

Multichelated compounds should, at least theoretically, also be more sensitive in detecting tumors with a very low receptor density, or very small tumors or metastases, since more radioactivity can be delivered per receptor molecule while uptake in non receptor-expressing background remains low. In addition, this approach may help to make radiotracers suitable for autoradiography studies as the detection limit of autoradiography is dependent on target saturation and thus limits the tracer amount used. Finally, the potential of non-internalizing peptides with antagonistic features for tumor detection might be increased by improving radioactivity accumulation (which is lower due to lack of internalization) in the target tissue.

In conclusion, despite slightly decreased relative uptake of the tracer in the pancreas in rats, our multichelator approach led to an increase in signal-to-background ratio as a result of the improved specific activity. The higher target organ radioactivity accumulation led to improved visibility of pancreatic tissue in SPECT images in rodents. This technology may represent a major asset for reliable quantitative measurements of BCM *in vivo* for diabetes research. Moreover, this approach has great potential for translation to other peptides and chelators/radionuclides, where it is essential to perform examination with high specific activity.

AUTHOR INFORMATION

Corresponding Author

*Telephone/Fax: +31 24 36 67319/+31 24 36 18942; E-mail: Lieke.Claessens-Joosten@radboudumc.nl.

ORCID

Lieke Joosten: 0000-0003-4427-8664

Sandra Heskamp: 0000-0001-7250-0846

Martin Béhé: 0000-0002-1110-2665

Present Address

[§]Maastricht Radiation Oncology (Maastricht) Lab, GROW—School for Oncology and Developmental Biology, Maastricht University Medical Center, Maastricht, The Netherlands

Notes

The authors declare no competing financial interest.

ACKNOWLEDGMENTS

We thank Bianca Lemmers, Kitty Lemmens, Iris Lamers-Elmans, and Henk Arnts (Central Animal Facility, Radboud University Medical Center, Nijmegen, The Netherlands) for their expertise in the *in vivo* studies. Our work was supported by NIH grant 1R01 AG 030328-01, the European Union's Seventh Framework Programme project BetaImage, under grant agreement No. 222980 and project BetaCure, under agreement No. 602812.

REFERENCES

- 1) <http://www.who.int/mediacentre/factsheets/fs312/en/>.
- 2) Gotthardt, M.; Eizirik, D. L.; Cnop, M.; Brom, M. Beta cell imaging - a key tool in optimized diabetes prevention and treatment. *Trends Endocrinol. Metab.* **2014**, *25*, 375–377.
- 3) Brom, M.; Andraojc, K.; Oyen, W. J. G.; Boerman, O. C.; Gotthardt, M. Development of radiotracers for the determination of the beta-cell mass in vivo. *Curr. Pharm. Des.* **2010**, *16*, 1561–1567.
- 4) Krogvold, L.; Edwin, B.; Buanes, T.; et al. Pancreatic biopsy by minimal tail resection in live adult patients at the onset of type 1 diabetes: experiences from the DiViD study. *Diabetologia* **2014**, *57*, 841–843.
- 5) Gotthardt, M. Beta cell imaging—why we need it and what has been achieved. *Curr. Pharm. Des.* **2010**, *16*, 1545–1546.
- 6) Eriksson, O.; Laughlin, M.; Brom, M.; et al. In vivo imaging of beta cells with radiotracers: state of the art, prospects and recommendations for development and use. *Diabetologia* **2016**, *59*, 1340–1349.
- 7) Andraojc, K.; Srinivas, M.; Brom, M.; et al. Obstacles on the way to the clinical visualisation of beta cells: looking for the Aeneas of molecular imaging to navigate between Scylla and Charybdis. *Diabetologia* **2012**, *55*, 1247–1257.
- 8) Goke, B. What are the potential benefits of clinical beta-cell imaging in diabetes mellitus? *Curr. Pharm. Des.* **2010**, *16*, 1547–1549.
- 9) Jodal, A.; Schibli, R.; Behe, M. Targets and probes for non-invasive imaging of beta-cells. *Eur. J. Nucl. Med. Mol. Imaging* **2017**, *44*, 712.
- 10) Moore, A. Advances in beta-cell imaging. *Eur. J. Radiol.* **2009**, *70*, 254–257.
- 11) Brom, M.; Woliner-van der Weg, W.; Joosten, L.; et al. Non-invasive quantification of the beta cell mass by SPECT with ¹¹¹In-labelled exendin. *Diabetologia* **2014**, *57*, 950.
- 12) Lankat-Buttgereit, B.; Goke, R.; Stockmann, F.; Jiang, J.; Fehmann, H. C.; Goke, B. Detection of the human glucagon-like peptide 1(7–36) amide receptor on insulinoma-derived cell membranes. *Digestion* **2004**, *55*, 29–33.
- 13) Reubi, J. C.; Waser, B. Concomitant expression of several peptide receptors in neuroendocrine tumours: molecular basis for in vivo multireceptor tumour targeting. *Eur. J. Nucl. Med. Mol. Imaging* **2003**, *30*, 781–793.
- 14) Brom, M.; Oyen, W. J.; Joosten, L.; Gotthardt, M.; Boerman, O. C. ⁶⁸Ga-labelled exendin-3, a new agent for the detection of insulinomas with PET. *Eur. J. Nucl. Med. Mol. Imaging* **2010**, *37*, 1345–1355.
- 15) Wild, D.; Behe, M.; Wicki, A.; et al. [¹²⁵I]exendin-4, a very promising ligand for glucagon-like peptide-1 (GLP-1) receptor targeting. *J Nucl Med.* **2006**, *47*, 2025–2033.
- 16) Thorkildsen, C.; Neve, S.; Larsen, B. D.; Meier, E.; Petersen, J. S. Glucagon-like peptide 1 receptor agonist ZP10A increases insulin mRNA expression and prevents diabetic progression in db/db mice. *J. Pharmacol. Exp. Ther.* **2003**, *307*, 490–496.
- 17) Brom, M.; Joosten, L.; Oyen, W. J.; Gotthardt, M.; Boerman, O. C. Improved labelling of DTPA- and DOTA-conjugated peptides and antibodies with ¹¹¹In in HEPES and MES buffer. *EJNMMI Res.* **2012**, *2*, 4.
- 18) Brom, M.; Franssen, G. M.; Joosten, L.; Gotthardt, M.; Boerman, O. C. The effect of purification of Ga-68-labeled exendin on in vivo distribution. *EJNMMI Res.* **2016**, *6*, 65.
- 19) Asfari, M.; Janjic, D.; Meda, P.; Li, G.; Halban, P. A.; Wollheim, C. B. Establishment of 2-mercaptoethanol-dependent differentiated insulin-secreting cell lines. *Endocrinology* **1992**, *130*, 167–178.
- 20) van Hooft, R. A.; Vriens, D.; Postema, J. W.; et al. The influence of SPECT reconstruction algorithms on image quality and diagnostic accuracy in phantom measurements and ^{99m}Tc-sestamibi parathyroid scintigraphy. *Nucl. Med. Commun.* **2014**, *35*, 64–72.
- 21) Breeman, W. A.; Jong, M.; Visser, T. J.; Erion, J. L.; Krenning, E. P. Optimising conditions for radiolabelling of DOTA-peptides with

^{90}Y , ^{111}In and ^{177}Lu at high specific activities. *Eur. J. Nucl. Med. Mol. Imaging* **2003**, *30*, 917–920.

(22) Heskamp, S.; Hobo, W.; Molkenboer-Kueneen, J. D.; et al. Noninvasive Imaging of Tumor PD-L1 Expression Using Radiolabeled Anti-PD-L1 Antibodies. *Cancer Res.* **2015**, *75*, 2928–2936.

(23) Heskamp, S.; van Laarhoven, H. W.; Molkenboer-Kueneen, J. D.; et al. ImmunoSPECT and immunoPET of IGF-1R expression with the radiolabeled antibody R1507 in a triple-negative breast cancer model. *J. Nucl. Med.* **2010**, *51*, 1565–1572.

(24) Boniface, G. R.; Izard, M. E.; Walker, K. Z.; et al. Labeling of monoclonal antibodies with samarium-153 for combined radio-immunoscintigraphy and radioimmunotherapy. *J Nucl Med* **1989**, *30*, 683–691.